

56<sup>TH</sup> ARFTG CONFERENCE DIGEST

FALL 2000



AUTOMATIC RF TECHNIQUES GROUP

*Metrology and Test for RF Telecommunications*

30 November & 01 December 2000

Boulder, Colorado

# 56<sup>TH</sup> ARFTG CONFERENCE DIGEST

## Preface

The 56<sup>TH</sup> ARFTG Conference was held 30 November and  
01 December 2000 at the Omni Interlocken Hotel  
Boulder, Colorado

Conference Theme:

"Metrology and Test for RF Telecommunications"

Conference Chair  
Technical Program Chairs

Dr. Dylan Williams  
Dr. Kate Remley  
Dr. Michael Steer

Publication Date  
Publication Chair

November 2000  
J.G. Burns

## Improving the Uncertainty Analysis of NIST's Pulse Parameter Measurement Service

N.G. Paulter  
D.R. Larson  
Electricity Division  
National Institute of Standards and Technology  
Gaithersburg, MD 20899

### Abstract:

A new uncertainty analysis is being performed for NIST's pulse parameter measurement service that represents the new pulse parameter measurement and extraction process. This new analysis is expected to have lower uncertainties compared to those presently reported.

### 1. Introduction

The National Institute of Standards and Technology (NIST) supports a measurement service for high-speed (transition durations,  $t_d < 20$  ps) pulse generators that provides an estimate of the pulse parameters of amplitude and transition duration [1]. NIST previously provided overshoot and undershoot (preshoot) parameters as well.

NIST is one of two national measurement laboratories that provide a pulse parameter measurement service; the other national laboratory is the National Physical Laboratory (NPL) in the United Kingdom. NIST and NPL are presently performing an intercomparison of pulse parameter results, which includes measured data, corrected data (if applicable), and reconstructed data. Thus far, the results indicate that both national laboratories are in close agreement.

The NIST measurement service presently uses commercially-available high-bandwidth sampling oscilloscopes (-3 dB attenuation bandwidths of approximately 50 GHz and 20 GHz) and pulse generators (- 3 dB attenuation bandwidths of approximately 20 GHz).

### 2. Measurement Process

The pulse parameter measurement process is briefly described in this section. An estimate of the impulse response of the NIST 20-GHz samplers is obtained using high-speed pulse generators and a 50 GHz sampler. The pulse measured by the 50 GHz sampler is taken for the reference. Note: we are examining the "nose-to-nose" method for estimating the impulse response of high bandwidth sampling oscilloscopes [2,3] and its limitations in performing the calibration of fast samplers.

Official contribution of the National Institute of Standards and Technology; not subject to copyright in the United States.

Several sets of data are acquired for the customer's pulse generator (or device under test, DUT). A set of data consists of a sampler-acquired DUT waveform, an estimate of the time-base errors [4-7], and a measurement of the dynamic gain (see Sec. 3.1) of the sampler.

The DUT waveforms are subsequently corrected for gain and time-base errors only if these errors are large relative to the other uncertainties. The corrected waveforms are then used in a reconstruction process to obtain a waveform that is an accurate estimate of the pulse delivered to the sampler. The accuracy of this estimate (the reconstructed waveform) is dependent on the reconstruction process and the accuracy of the estimate of the sampler impulse response. From each reconstructed waveform, pulse parameter values are extracted. The set of pulse parameter values thus extracted is used to determine the mean value and standard deviation for the given parameter

### 3. Uncertainty Analysis

The reported pulse parameters are an average of the particular pulse parameters obtained from a set of  $M_1$  pulse waveforms measured using the NIST pulse measurement systems. The average of a parameter,  $W$  for example, is given by:

$$\langle W \rangle = \frac{1}{M} \sum_{i=1}^M W_i(\alpha_j), \quad (1)$$

where  $M$  is the number of values for the parameter  $W$ , one value for each waveform, and  $W$  is dependent on a number,  $N$  of variables,  $\alpha_j$ . The standard uncertainty for this average,  $\langle W \rangle$  for example, is given by:

$$\begin{aligned} u_{\langle W \rangle} &= \sqrt{\sum_{i=1}^M \left[ \left( \frac{\partial \langle W \rangle}{\partial W_i} \right)^2 \sum_{j=1}^N \left( \frac{\partial W_i(\alpha_j)}{\partial \alpha_j} \right)^2 u_{\alpha_j}^2 \right]} \\ &= \sqrt{\sum_{i=1}^M \left[ \frac{1}{M^2} \sum_{j=1}^N \left( \frac{\partial W_i(\alpha_j)}{\partial \alpha_j} \right)^2 u_{\alpha_j}^2 \right]} \quad (a) \\ &= \sqrt{\frac{1}{M} \sum_{j=1}^N \left( \frac{\partial W(\alpha_j)}{\partial \alpha_j} \right)^2 u_{\alpha_j}^2} \quad (b) \end{aligned} \quad (2)$$

where it is assumed in (2a) that the  $\alpha_j$  are uncorrelated, which is the reason there are no cross terms in the partial derivatives with respect to the  $\alpha_j$ . In (2b) it is further assumed that the  $u_{\alpha_j}$  are

the same for each  $W_i$ ; that is, the uncertainties in the variables for a given parameter are the same for each waveform.

### 3.1 Pulse amplitude

The pulse amplitude, as are all the pulse parameters, is obtained using a histogram-based algorithm. Calculating the uncertainty in the pulse amplitude requires having an equation that describes the reported pulse amplitude,  $V_A$ :

$$V_A = \frac{\langle V_{A,c} + V_{\Delta T} \rangle_{M_1}}{g} = (\bar{V}_{A,c} + \bar{V}_{\Delta T}) / g, \quad (3)$$

where “ $\langle \rangle$ ” indicates an average (as do the horizontal bars above a variable),  $\bar{V}_{A,c}$  is the average of the set of  $M_1$  pulse amplitudes corrected for sampler offset errors,  $\bar{V}_{\Delta T}$  is the average of the amplitude corrections required for a change in measurement temperature, and  $g$  is the dynamic gain of the sampler. The dynamic gain is affected by the impulse response of the sampler and the waveform epoch because the impulse response of a sampler is always a decaying function of time. If this decay time is longer in duration than the waveform epoch used, then the measured signal (a step) would not reach its static (steady-state) high level. The dynamic gain is determined by comparing the pulse amplitude of a reference pulse as measured using a reference instrument[9] and the sampler for the same epoch.

The temperature correction term is obtained by measuring the change in the observed pulse amplitude with temperature [8]. The dynamic gain term,  $g$ , is obtained by taking the ratio of the amplitude of the reference pulse as measured using the sampler and the amplitude of the reference pulse as measured using a reference instrument[9], which in our case, is a high-accuracy, high-bandwidth (-3 dB attenuation bandwidth > 1 GHz) .

In general, the standard uncertainty of a function,  $W(\alpha_1, \alpha_2, \alpha_3, \dots, \alpha_M)$ , of  $M$  independent variables,  $\alpha$ , is given by:

$$u_{W(\alpha_1, \alpha_2, \dots, \alpha_M)} = \sqrt{\sum_{i=1}^M \left( \frac{\partial W(\alpha_1, \alpha_2, \dots, \alpha_M)}{\partial \alpha_i} \right)^2 k_{\alpha_i}^2 u_{\alpha_i}^2}, \quad (4)$$

where the  $k$  is the statistical weight [10] applied to the uncertainties of variables obtained from a limited number of trials. The uncertainties in these variables,  $u_i$  (where the “ $i$ ” subscript refers to a parameter) are obtained from independent measurements that provide values for those particular variables. A partial list of potential contributors to pulse parameter uncertainty are: high and low state levels, measurements used to calculate the dynamic gain, the histogram parameters, and temperature dependencies. To calculate the uncertainty of  $V_A$ , the partial derivatives of  $V_A$  with respect to the independent variables must also be calculated. In addition,

the uncertainty of each variable must be appropriately weighted to reflect the number of times a measurement was performed to calculate the value of that variable [10].

In addition to measurement-related uncertainties, the reported amplitude values are also subject to uncertainties from the method used to calculate these values that, in this case, is a histogram method.

### 3.2 Transition Duration

The reported (and therefore, reconstructed waveform) transition duration,  $t_d$ , is the average transition duration extracted from  $M_1$  reconstructed pulse waveforms.  $t_d$  is related to the transition duration of the measured waveform,  $t_{d,m}$ , and the transition duration of the sampler step response,  $t_{d,r}$ :

$$t_d = \left\langle f(t_{d,m}, t_{d,r}, T) \right\rangle_{M_1}, \quad (5)$$

where  $T$  is temperature. The specific functional relationship between  $t_d$ ,  $t_{d,m}$ , and  $t_{d,r}$ , however, is dependent on the type of waveforms used. For example, for Gaussian waveforms,  $t_d$  is equal to the square root of the difference of the squares of transition durations of the measured and step response waveforms. We can write an equation describing  $t_d$  as:

$$\begin{aligned} t_d &= \left\langle t_{d,R} \right\rangle_{M_1} \\ &= \left\langle t_{d,m} *^{-1} t_{d,r} + \Delta t_{d,\Delta T} \right\rangle_{M_1}, \end{aligned} \quad (6)$$

where “ $*^{-1}$ ” is used to indicate that  $t_d$  is found from a waveform that is obtained by deconvolving a waveform with transition duration  $t_{d,r}$  from a waveform with transition duration  $t_{d,m}$ . The  $\Delta t_{d,\Delta T}$  is the temperature-induced incremental change in transition duration [8]. Since we do not know, a priori, the functional relationship, we obtain an empirical relationship relating the three parameters. We obtain this relationship by fitting a curve (such as a polynomial) to  $t_{d,m}$ -vs- $t_d$  data and separately to  $t_{d,r}$ -vs- $t_d$  data where both  $t_{d,m}$  and  $t_{d,r}$  are varied within expected values and the  $t_d$  is obtained from the reconstructed waveforms. The  $t_{d,m}$  and  $t_{d,r}$  are determined by linearly interpolating to obtain the instant in time (the reference level instant) corresponding to the given reference level. Typical reference levels are 10 % and 90 % of pulse amplitude.

A partial list of potential contributors to transition duration uncertainty are: high and low state levels, measurements used to calculate the dynamic gain, the histogram parameters, pulse amplitude, the interpolation process, and temperature dependencies.

### 3.3 Overshoot and under(pre)shoot

Voltage offset errors will not be considered here because they will cancel as they did for the uncertainty calculation of  $V_{A,c}$ . The equation describing the calculation for the overshoot is:

$$OS = \left\langle \frac{V_{\max,R}(t_d) - V_{S2,R}}{V_{A,R}} \right\rangle_{M_1}, \quad (7)$$

where the brackets, “< >,” indicate an average value and ( $t_d$ ) is meant to imply a restricted temporal region of the waveform which is a function of the transition duration. The subscript “R” indicates that the voltage V was obtained using a reference instrument and S2 refers to the second state level, which is usually the topline. The percentage overshoot is obtained by multiplying (9) and 100 %. An analogous expression can be obtained for the undershoot parameter.

A partial list of potential contributors to overshoot/undershoot uncertainty are: high and low state levels, measurements used to calculate the dynamic gain, the histogram parameters, pulse amplitude, and temperature dependencies.

### 3.4 Temperature Effects

The temperature at which the measurements are taken affect both observed pulse amplitude and transition duration (see curves labeled “SH” in figs. 1 and 2). These figures show that the impulse response of the samplers, for both manufacturers of high-speed sampling oscilloscopes, is affected by temperature and that the trends for both these parameters with temperature and for both manufacturers is approximately linear. Consequently, a functional relationship, namely a best fit straight line, between these parameters and temperature can be obtained and used to correct those parameters for temperature variations.

### 3.5 Reference Pulse

One of the most difficult problems in calibrating the measurement system is obtaining an accurate estimate of the impulse response of the sampler. Several methods have been described in the literature [3,11,12] but none have been proven to be adequate for calibration-quality measurements. The nose-to-nose method [3] for example, requires that the sampler behave identically as pulse generator and sampler and that the magnitude of the so-called “kick-out” pulse be the same independent of polarity of a control variable, the offset voltage. We have observed that this assumption is not true [13]. However, we have not yet ascertained whether this deviation will introduce significant error into our reported pulse parameters. This assessment requires a complete uncertainty analysis of the measurement process, a part of which is presented here. Other techniques that have been used to approximate the impulse response or magnitude of the transfer function of the sampler include optoelectronic methods and swept frequency methods [11]. The degree of agreement between these methods is frequency dependent and, in general, not close [11, 14]. The swept frequency methods, to date, only provide the magnitude of the sampler’s transfer function.

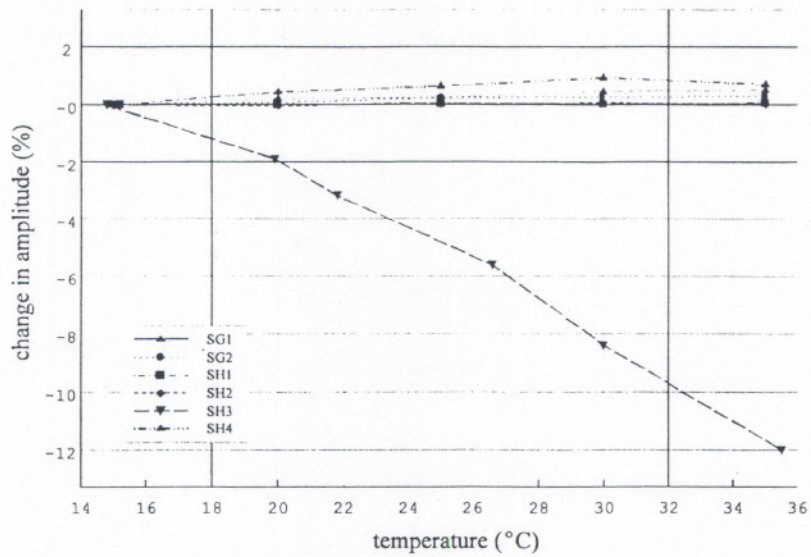


Figure 1. The percent change in pulse amplitude with temperature relative to 15 °C.

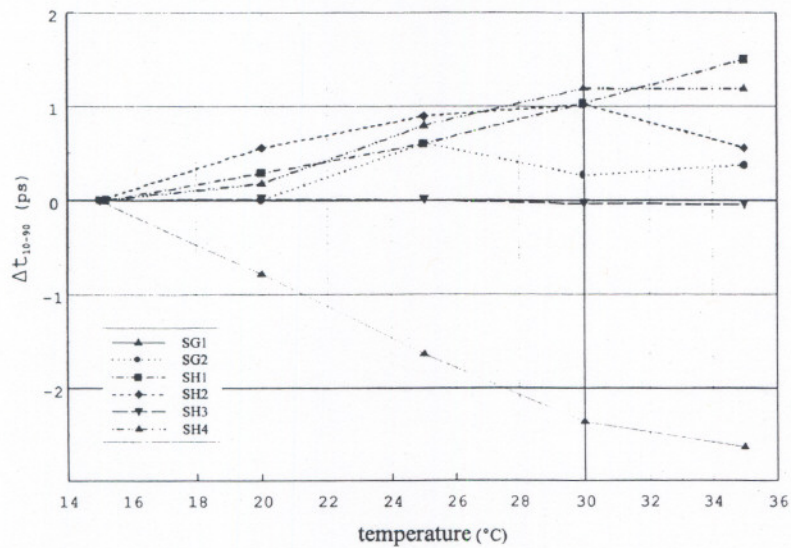


Figure 2. The change in transition duration,  $\Delta t_{10-90}$ , with temperature relative to 15 °C.

The uncertainty in impulse response, independent of the method from which it is obtained, must be tracked to the reported pulse parameters. Typically, an estimate of the input pulse is obtained via a reconstruction process, which involves a division of the spectra of the measured waveform

by the impulse response and then some type of filtering. The filtering is necessary because the deconvolution is an ill-posed problem [15-21] and the reconstructed signal may exhibit large oscillations (with amplitudes frequently hundreds of times greater than the amplitude of the measured pulse) unless filtered. In regularized reconstructions, the filter includes the sampler impulse response estimate. Therefore, the uncertainties of the impulse response estimate must be tracked through a time-to-frequency transformation, a spectral division, filtering, and then a frequency-to-time transformation; or an empirical relationship between the pulse parameters and the impulse response estimate be found.

The reference pulse may also exhibit temperature and other dependencies. We have observed a temperature dependence in the pulse generators (see curves labeled "SG" in figs. 1 and 2). The pulse generator output may also exhibit a repetition-rate or duty-factor dependence. Although we have observed this type of dependence in measured waveforms, we simply noted it as an anomaly and did not identify if the dependence was due to the sampler or the pulse generator.

### **3. Status of Work**

The uncertainty analysis of the NIST pulse parameter measurement service is nearly complete: the equations describing the functional dependence of the pulse parameters on measurement variables have been determined, auxiliary measurements (time-base error, gain error, etc.) required for calibration have been determined, and methods for extracting empirical relationships between the pulse parameters and certain measurement variables has been determined. Determining the uncertainties in the impulse response estimate has yet to be completed. The effect of these uncertainties on the pulse parameters will, more than likely, be determined by obtaining an empirical relationship between the pulse parameter and the impulse response estimate.

### **Acknowledgments**

We would like to P.D. Hale of NIST, Boulder, CO and W.F. Guthrie of NIST-Gaithersburg, MD for reviewing this paper and providing technical comments. We are also thankful to B.A. Bell of NIST-Gaithersburg for editorial administrative support.

### **References**

1. NIST Calibration Services Users Guide, NIST Special Publication, SP250, U.S. Department of Commerce, Washington, DC, January 1998, pp. 189-193.
2. K. Rush, S. Draving, and J. Kerley, "Characterizing high-speed oscilloscope," IEEE Spectrum, September 1990, pp. 38-39.
3. J. Verspecht, "Broadband sampling oscilloscope characterization with the 'nose-to-nose' calibration procedure: A theoretical and practical analysis," IEEE Trans. Instrum. Meas., Vol. 44, December 1995, pp. 991-997.

4. J. Verspecht, "Accurate spectral estimation based on measurements with a distorted-timebase digitizer," *IEEE Trans. Instrum. Meas.*, Vol. 43, April 1994, pp. 210-215.
5. R. Pintelon and J. Schoukens, "An improved sine-wave fitting procedure for characterizing data acquisition channels," *IEEE Trans. Instrum. Meas.*, Vol. 45, April 1996, pp. 588-593.
6. G.N. Stenbakken and J.P. Deyst, "Time-base nonlinearity determination using iterated sine-fit analysis," *IEEE Trans. Instrum. Meas.*, Vol. 47, October 1998, pp. 1056-1061.
7. C.M. Wang, P.D. Hale, and K.J. Coakley, "Least-squares estimation of time-base distortion of sampling oscilloscopes," *IEEE Trans. Instrum. Meas.*, Vol. 48, December 1999, pp. 1324-1332.
8. D.R. Larson and N.G. Paulter, "Temperature effects on the high-speed response of digitizing sampling oscilloscopes," *NCSL International, 2000 Workshop and Symposium, Toronto, Canada, 16-20 July 2000.*
9. T.M. Souders, B.C. Waltrip, O.B. Laug, and J.P. Deyst, "A wideband sampling voltmeter," *IEEE Trans. Instrum. Meas.*, Vol. 46, August 1997, pp. 947-953.
10. B.N. Taylor and C.E. Kuyatt, NIST Technical Note 1297, "Guidelines for evaluating and expressing the uncertainty of NIST measurement results," U.S. Dept. of Commerce, 1994.
11. D. Henderson, A.G. Roddie, and A.J.A. Smith, "Recent developments in the calibration of fast sampling oscilloscopes," *IEE Proceedings-A*, Vol. 139, September 1992, pp. 254-260.
12. A.J.A. Smith, A.G. Roddie, and D. Henderson, "Electrooptic sampling of low temperature GaAs pulse generators for oscilloscope calibration," *Optical and Quantum Elec.*, Vol. 28, 1996, pp. 933-944.
13. D.R. Larson and N.G. Paulter, "The effect of offset voltage on the kick-out pulses used in the nose-to-nose sampler impulse response characterization method," *IEEE Instrumentation and Measurement Technology Conference, Proceedings, Baltimore, USA, 1-4 May 2000*, pp. 1425-1428.
14. P.D. Hale, T.S. Clement, K.J. Coakley, C.M. Wang, D.C. DeGroot, and A.P. Verdoni, "Estimating the magnitude and phase response of a 50 GHz sampling oscilloscope using the 'nose-to-nose' method," *Automatic Radio Frequency Techniques Group, 55<sup>th</sup> ARFTG Conference Digest, Boston, USA, June 2000.*
15. A.N. Tikhonov and V.Y. Arsenin, *Solutions of Ill-posed Problems*, V.H. Winston & Sons, Washington, DC, 1977.
16. K. Miller, "Least squares methods for ill-posed problems with a prescribed bound," *SIAM J. Math. Anal.*, Vol.1, February 1970, pp. 53-75.

17. N.S. Nahman and M.E. Guillaume, "Deconvolution of time domain waveforms in the presence of noise," National Bureau of Standards Tech. Note 1047, U.S. Department of Commerce, Washington, DC , 1981.
18. N.G. Paulter, "A causal regularizing deconvolution filter for optimal waveform reconstruction," IEEE Trans. Instrum. Meas., Vol. 43, October 1994, pp. 740-747.
19. T. Daboczi, "Uncertainty of signal reconstruction in the case of jittery and noisy measurements," IEEE Trans. Instrum. Meas., Vol. 47, October 1998, pp. 1062-1066.
20. T. Daboczi and I. Kollar, "Multiparameter optimization of inverse filtering algorithms," IEEE Trans. Instrum. Meas., Vol. 45, April 1996, pp. 417-421.
21. S. Roy and T.M. Souders, "Non-iterative waveform deconvolution using analytic reconstruction filters with time-domain weighting," IEEE Instrumentation and Measurement Technology Conference, Proceedings, Baltimore, USA, 1-4 May 2000.